Ann. Geophys., 27, 2861–2867, 2009
www.ann-geophys.net/27/2861/2009/

Annales Geophysicae

Comparing daytime, equatorial $E \times B$ drift velocities and TOPEX/TEC observations associated with the 4-cell, non-migrating tidal structure

D. Anderson[1,2], **E. Araujo-Pradere**[1,2], **and L. Scherliess**[3]

[1]Cooperative Institute for Research in Environmental Sciences, University of Colorado, USA
[2]Space Weather Prediction Center, National Centers for Environmental Prediction, National Weather Service, National Oceanic and Atmospheric Administration, Boulder, CO, USA
[3]Center for Atmospheric and Space Sciences, Utah State University, Logan, UT, USA

Received: 26 September 2008 – Revised: 20 March 2009 – Accepted: 20 March 2009 – Published: 20 July 2009

Abstract. We investigate the seasonal and longitude dependence of the daytime, vertical $\boldsymbol{E} \times \boldsymbol{B}$ drift velocities, on a day-to-day basis, using a recently-developed technique for inferring realistic $\boldsymbol{E} \times \boldsymbol{B}$ drifts from ground-based magnetometer observations. We have chosen only quiet days, $A_p < 10$, from January 2001 through December 2002, so that the main contribution to the variability is due to the variability in the tidal forcing from below. In order to study the longitude dependence in daytime $\boldsymbol{E} \times \boldsymbol{B}$ drift velocities, we use appropriately-placed magnetometers in the Peruvian, Philippine, Indonesian and Indian longitude sectors. Since we are particularly interested in quantifying the $\boldsymbol{E} \times \boldsymbol{B}$ drift velocities associated with the 4-cell, non-migrating tidal structure, we compare the seasonal and longitude $\boldsymbol{E} \times \boldsymbol{B}$ drift structure with TOPEX satellite observations of Total Electron Content (TEC). We outline a plan to establish the magnitude of the longitude gradients that exist in the daytime, vertical $\boldsymbol{E} \times \boldsymbol{B}$ drift velocities at the boundaries of the observed 4-cell patterns and to theoretically identify the physical mechanisms that account for these sharp gradients. The paper demonstrates that sharp gradients in $\boldsymbol{E} \times \boldsymbol{B}$ drift velocities exist at one of the 4-cell boundaries and outlines how the C/NOFS IVM and VEFI sensor observations could be used to establish the $\boldsymbol{E} \times \boldsymbol{B}$ drift longitude gradients at the boundaries of each of the 4 cells. In addition, the paper identifies one of the theoretical, atmosphere/ionosphere models that could be employed to identify the physical mechanisms that might explain these observations.

Keywords. Ionosphere (Electric fields and currents; Equatorial ionosphere; Ionosphere-atmosphere interactions)

Correspondence to: D. Anderson
(david.anderson@noaa.gov)

1 Introduction

In the Earth's ionospheric F-region, between 200 and 800 km altitude, the daytime distribution of electrons and ions as a function of altitude, latitude, longitude and local time are determined by ionospheric production, loss and transport mechanisms. Production is primarily through photo-ionization of atomic oxygen by solar EUV radiation, $\lambda < 91.1$ nm and loss is through charge exchange of O^+ ions with N_2 and O_2, to give NO^+ and O_2^+, followed by recombination with electrons. Transport of ionization perpendicular to B is due to $\boldsymbol{E} \times \boldsymbol{B}$ drifts and transport parallel to B is due to ambipolar diffusion and the component of the neutral wind parallel to B. At low latitudes, the primary transport mechanism is via $\boldsymbol{E} \times \boldsymbol{B}$ drifts in the vertical and meridional plane. At the magnetic equator, these $\boldsymbol{E} \times \boldsymbol{B}$ drifts are upward in the daytime and primarily downward at night. The daytime upward drifts are responsible for producing crests in the F-region peak electron density, Nmax, at ± 15 to 18° magnetic latitude, known as the equatorial anomaly (Hanson and Moffett, 1966; Anderson, 1973).

It is well known that diurnal and semi-diurnal tides in the E-region cause positive ions to move relative to the electrons (which are fixed to geomagnetic field lines) through collisions with neutrals, thus setting up a current that must be divergence free. To do this, polarization electric fields are set up and this process is known as the "E-region wind dynamo". Primarily, in the equatorial, daytime E- and F-region these polarization electric fields are eastward giving rise to upward, vertical $\boldsymbol{E} \times \boldsymbol{B}$ drifts that produce the F-region equatorial anomaly mentioned in the previous paragraph.

Recently, several observational studies have identified the existence of a 4-cell pattern in low latitude, ionospheric parameters with longitude that are primarily associated with

Published by Copernicus Publications on behalf of the European Geosciences Union.

the equinoctial season. The first evidence emerged from IMAGE satellite FUV (135.6 nm) radiance observations after sunset (20:00 LT) that clearly showed enhancements in airglow-inferred Nmax values at the crests of the equatorial anomaly in 4 specific longitude zones during March–April 2001 (Sagawa et al., 2005; Immel et al., 2006). The latter study attributed the 4-cell pattern to the effects of a 4-cell pattern in daytime, vertical $\boldsymbol{E}\times\boldsymbol{B}$ drift velocities associated with the diurnal, eastward propagating, non-migrating, wave number 3 (DE3) tidal mode (Hagan and Forbes, 2002) that have their origin due to deep tropical convection and latent heat release at tropospheric heights. A recent paper by Forbes et al. (2008) examines in detail the tidal variability in the dynamo region, the migrating and non-migrating diurnal (DE3) tides and gives a succinct explanation for the relation between ground-based and space-based perspectives of atmospheric tides.

Since the IMAGE observations were at night, Immel et al. (2006) could not rule out a 4-cell pattern in the pre-reversal enhancement in $\boldsymbol{E}\times\boldsymbol{B}$ drift that occurs after sunset. A subsequent paper by England et al. (2006), however, established that the 4-cell pattern was observed in CHAMP satellite in-situ electron densities at 12:00 LT. Further, the 4-cell pattern has also been observed in ROCSAT-1, daytime electron densities and $\boldsymbol{E}\times\boldsymbol{B}$ drift velocities at 600 km (Kil et al., 2007; Fejer et al., 2008) and COSMIC occultation observations (Lin et al., 2007). While Kil et al. (2007) find a 4-cell structure in daytime $\boldsymbol{E}\times\boldsymbol{B}$ drift velocities, this study averaged over the years from 1999 to 2004 and over season and did not determine seasonal variability or the longitude gradients in $\boldsymbol{E}\times\boldsymbol{B}$ drift that define the edges of the individual cells. However, Fejer et al. (2008) also analyzing ROCSAT-1 observations of daytime and nighttime $\boldsymbol{E}\times\boldsymbol{B}$ drift velocities at 600 km find daytime $\boldsymbol{E}\times\boldsymbol{B}$ drift velocities with a strong wave-number 4 signature in the Equinox and June solstice periods. They present the longitude gradients in these daytime $\boldsymbol{E}\times\boldsymbol{B}$ drift velocity signatures.

This current study is important and unique in that it is the first investigation to specifically 1.) Relate observed, ground-based, daytime $\boldsymbol{E}\times\boldsymbol{B}$ drift velocities with TOPEX-observed 4-cell TEC structures, 2.) Determine the sharp longitude gradients in $\boldsymbol{E}\times\boldsymbol{B}$ drift velocities that are responsible for the sharp gradients in observed TEC values, 3.) Study, for the first time, the seasonal dependence in observed $\boldsymbol{E}\times\boldsymbol{B}$ drifts at 4 longitudes and how they can explain the seasonal/longitude dependence in the TOPEX-observed TEC values, and 4.) Outline a plan to incorporate both observations and theoretical models to further our understanding of the physical mechanisms that are responsible for the 4-cell structure.

In this paper, we incorporate recently-developed techniques that use ground-based magnetometer observations to infer daytime, vertical $\boldsymbol{E}\times\boldsymbol{B}$ drift velocities and relate these $\boldsymbol{E}\times\boldsymbol{B}$ drifts to TOPEX TEC observations (Scherliess et al., 2008) in 4 longitude sectors under Equinoctial, June and December solstice conditions. The next "Data" section briefly describes 1.) The ground-based magnetometer technique for inferring daytime, vertical $\boldsymbol{E}\times\boldsymbol{B}$ drifts velocities and 2.) The TOPEX observational database (Scherliess et al., 2008). This is followed by a "Results" section in which we compare the TOPEX observations with the "average" $\boldsymbol{E}\times\boldsymbol{B}$ drift velocity vs local time curves for the 3 seasons in 2001 and 2002. We conclude with a "Conclusions and Future Work" section.

2 Data

A recent technique has been developed to infer the daytime, vertical $\boldsymbol{E}\times\boldsymbol{B}$ drift velocity from ground-based magnetometer observations (Anderson et al., 2002). Utilizing a magnetometer located on the magnetic equator (Jicamarca, Peru) and one off the magnetic equator at 6° N mag. lat. (Piura, Peru), Anderson et al. (2004) developed various relationships between the observed difference in the H component, ΔH ($H_{\rm Jic}$–$H_{\rm Piura}$), and the vertical $\boldsymbol{E}\times\boldsymbol{B}$ drift velocity observed by the JULIA (Jicamarca Unattended Long-term Ionosphere Atmosphere) coherent scatter radar measuring the Doppler shift of 150 km echo returns. These 150 km $\boldsymbol{E}\times\boldsymbol{B}$ drifts have been shown to be essentially equivalent to F-region $\boldsymbol{E}\times\boldsymbol{B}$ drift velocities by comparing them with the Jicamarca ISR (Incoherent Scatter Radar) $\boldsymbol{E}\times\boldsymbol{B}$ drifts. Anderson et al. (2004) developed a neural network technique that gave realistic, daytime $\boldsymbol{E}\times\boldsymbol{B}$ drift velocities. The neural network was trained with over 450 quiet and disturbed days between 2001 and 2004, using 5 min observations of ΔH and JULIA $\boldsymbol{E}\times\boldsymbol{B}$ drift velocities between 09:00 and 16:00 LT. A subsequent paper by Anderson et al. (2006), demonstrated that realistic $\boldsymbol{E}\times\boldsymbol{B}$ drift velocities could be obtained with the Peruvian sector-trained neural network, when applied to other longitude sectors where appropriately-placed magnetometers existed, such as in the Philippine and Indian sectors.

Figure 1 displays the magnetometer-inferred, daytime $\boldsymbol{E}\times\boldsymbol{B}$ drift velocities for quiet days ($A_p<10$) during the equinoctial period in the Peruvian (top figure), the Philippine (right figure) and the Indian (bottom figure) sectors. For the Peruvian sector, all of the 165 days are displayed as thin colored lines, where the thick red line is the average curve for all 165 days. This is compared to the thick blue line which is the Scherliess-Fejer (1999) climatological $\boldsymbol{E}\times\boldsymbol{B}$ drift curve. Similarly, for the Philippine sector, all of the 129 quiet days are displayed along with the average curve and for the Indian sector, all of the 92 days are displayed along with the average curve and each is compared to the Scherliess-Fejer climatological curve. The excellent comparisons give us confidence that realistic $\boldsymbol{E}\times\boldsymbol{B}$ drifts can be obtained from the ΔH technique.

We have compared the "average" magnetometer-inferred, daytime $\boldsymbol{E}\times\boldsymbol{B}$ drift velocities with the Scherliess-Fejer (1999) climatological $\boldsymbol{E}\times\boldsymbol{B}$ drift model, because this analytic model is the accepted climatological model that has

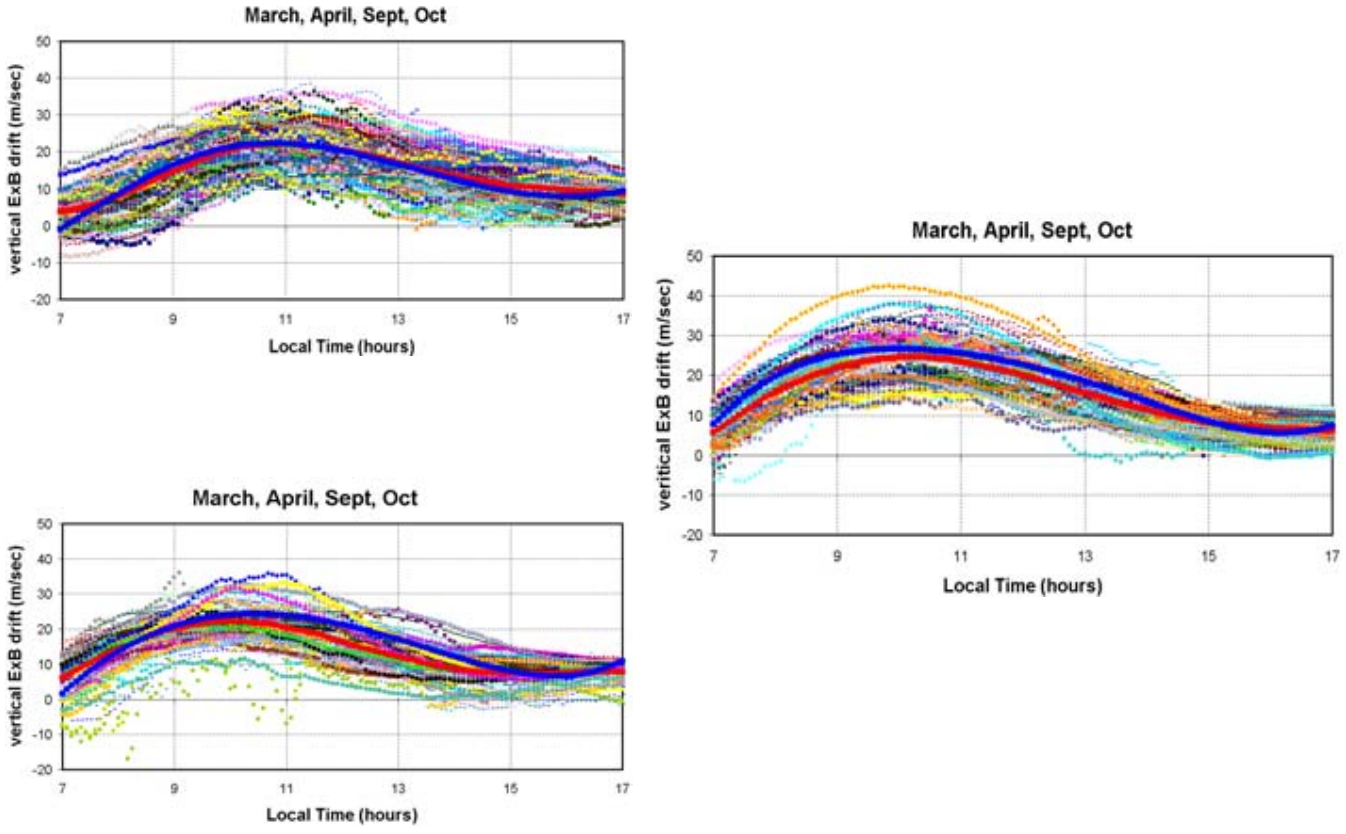

Fig. 1. Average ΔH-inferred $\boldsymbol{E}\times\boldsymbol{B}$ drifts (red curve) compared with the Scherliess-Fejer climatological model (blue curve) in the Peruvian (top), Philippine (right figure) and Indian (bottom) longitude sectors. The thin line colored curves in each figure represent individual, quiet day curves for each sector – Peruvian (165 days), Philippine (129 days) and Indian (92 days) (see text for details).

been used extensively to model equatorial ionospheric processes (Fejer et al., 2008). In the recent paper by Fejer et al. (2008), they have used five years of ROCSAT-1 $\boldsymbol{E}\times\boldsymbol{B}$ drift observations to develop a quiet-time, equatorial F-region plasma drift model. They find excellent agreement between this model and the Jicamarca Incoherent Scatter Radar (ISR) $\boldsymbol{E}\times\boldsymbol{B}$ drift observations. They also state that this ROCSAT-1 model is in good agreement with the Scherliess-Fejer model (1999), especially during the Equinox season, which implies that our comparison with the Scherliess-Fejer climatological model in the Peruvian, Philippine, and Indian sectors substantiates the realism of the ΔH-inferred $\boldsymbol{E}\times\boldsymbol{B}$ drift velocity technique.

The TOPEX/Poseidon satellite incorporates a dual-frequency altimeter operating at 13.6 GHz and 5.3 GHz to observe ocean surface heights. The dual-frequency allows the total electron content (TEC) to be measured from the satellite altitude of 1336 km to the ocean surface. The data set of TEC observations studied by Scherliess et al. (2008) covers the period from August 1992 until October 2005. For the current study a subset of their database has been used covering the years 2001–2002. As discussed by Scherliess et al. (2008) difficulties arise for a statistical analysis of the TOPEX TEC values due to the slow precession of the satellite orbit (2°/d). In their paper, Scherliess et al. normalized the TEC data to a common baseline in order to circumvent this problem and the same normalization has been applied in the current paper. In a nutshell, the normalization is accomplished by first finding the maximum TEC value for each ascending and descending pass between $\pm 30°$ geomagnetic latitude. Next, the peak values are longitudinally averaged to give daily values, again for ascending and descending passes, separately. These daily values were used as normalization factors, where each 18 s TEC data point was divided by its corresponding normalization factor. More detail concerning this applied normalization is given in Scherliess et al. (2008). The figures in this paper refer to "relative" TEC values that have been "normalized" using these factors.

3 Results

In this section we present the TOPEX TEC quiet-day observations binned by season and longitude for the years 2001 and 2002 and compare these observations with the quiet-day ΔH-inferred, daytime $\boldsymbol{E}\times\boldsymbol{B}$ drift velocities in 4 longitude

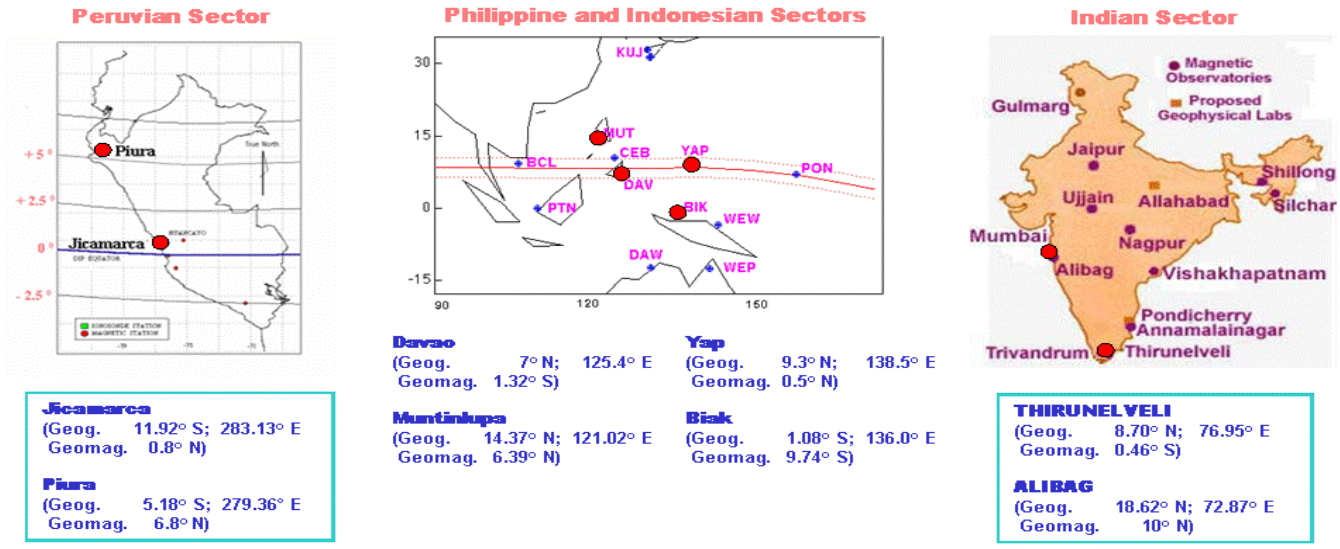

Fig. 2. The geomagnetic coordinates for the Peruvian, Philippine, Indonesian and Indian magnetometer locations.

sectors and averaged over the same seasonal periods in 2001 and 2002. Figure 2 displays the locations of the magnetometers in the Peruvian, Philippine, Indonesian and Indian sectors where the ground-based magnetometer observations have been used to infer the daytime, vertical $E \times B$ drift velocities for the 3 seasons in 2001 and 2002. Figure 3 presents the comparisons for the Equinoctial period while Figs. 4 and 5 present the comparisons for June and December solstice periods, respectively.

Figure 3a presents the average, daytime vertical $E \times B$ drift velocities as a function of local time in 4 longitude sectors for Equinox periods in 2001 and 2002. Note the large difference in maximum $E \times B$ drift velocity between the Philippine sector and the Indonesian sector, 23 m/s vs. 15 m/s. These two locations are only 15 degrees apart in longitude. In Fig. 3b, the TOPEX/TEC values are plotted for Equinox, 2001 and 2002, between 12:00 and 16:00 LT. The top portion of Fig. 3b displays the relative TEC values vs. longitude at the geomagnetic equator (red curve) and at 15° magnetic latitude (black curve). The values correspond to an average over of the Northern and Southern Hemisphere relative TEC values. The bottom portion of Fig. 3b is simply the average of the Northern and Southern Hemisphere relative TEC values plotted as a function of geographic longitude and absolute value of the geomagnetic latitude, to emphasize the location of the longitude gradients and the latitude crest separations. The longitude locations of the Peruvian (blue), Philippine (red), Indonesian (purple) and Indian (green) are indicated as vertical lines in the figure. The color of the vertical lines corresponds to the colored curves in Fig. 3a.

Referring to the top portion of Fig. 3b, there clearly exist 4 maxima in relative TEC at ∼0°, 100°, 190°, and 260° E geog. long. as Scherliess et al. (2008) have pointed out. The edges of the cells occur where the TEC values at the magnetic equator (red curve) come closest to or intersect the 15° mag. lat. TEC values (black curve). These longitudes are roughly at 50°, 150°, 220°, and 300° E geog. long. The "sharpness" of the cell boundary with longitude can be seen in how rapidly the TEC values at 15° and 0° mag. lat. converge. Note that between the Philippine sector (∼125° E geog. long.) and the Indonesian sector (∼140° E geog. long.), the TEC (15°) value is rapidly approaching the TEC (0°) value. The sharpness of this cell boundary is presumably related to the large difference in the maximum $E \times B$ drift velocities between the Philippine and Indonesian sectors displayed in Fig. 3a. Referring to Fig. 3b, there also appear to be sharp longitude gradients at 220° E and 320° E which would imply sharp gradients in the daytime, vertical $E \times B$ drift velocities at these longitudes, although these measurements have yet to be made.

In the June solstice period, Fig. 4b shows that the 4-cell pattern still persists, but to a much lesser degree. The maxima of the TEC values occur at the same longitudes and the minima also occur at the same longitudes as displayed in Fig. 3b for the Equinox period. With the exception of the 100° E long. sector, what is striking about the June solstice compared with the Equinox period is that the relative TEC values at the magnetic equator and at 15° mag. lat. are much closer to each other. This means that the equatorial anomaly crests in TEC are closer to the magnetic equator during the June solstice period which implies that the daytime, upward $E \times B$ drift velocities are smaller during June solstice than during Equinox. This is exactly what is observed when Fig. 4a is compared with Fig. 3a – a substantial decrease in $E \times B$ drift velocities at all 4 longitudes.

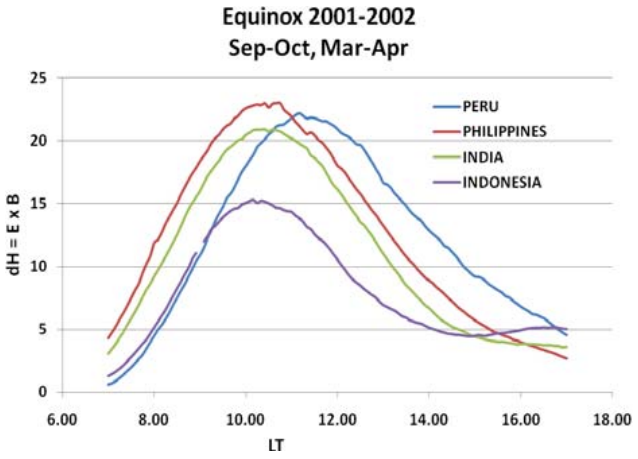

Fig. 3a. Average $E \times B$ drifts for Equinox 2001–2002 in the Peruvian, Philippine, Indonesian and Indian sectors (see text for details).

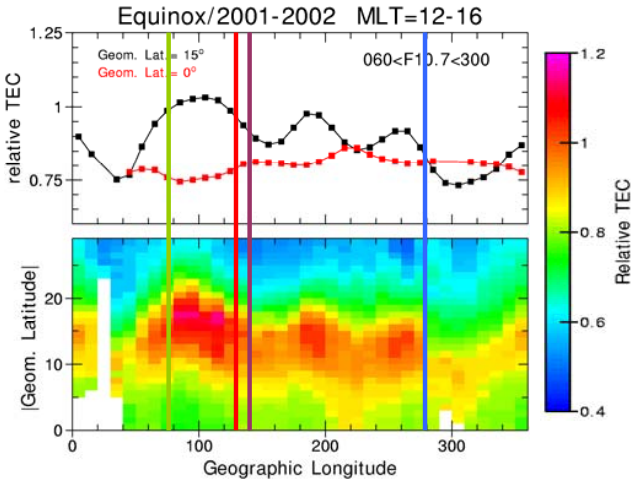

Fig. 3b. TOPEX relative TEC as a function of geographic longitude and magnetic latitude for Equinox 2001–2002 and 12:00–16:00 LT (see text for details).

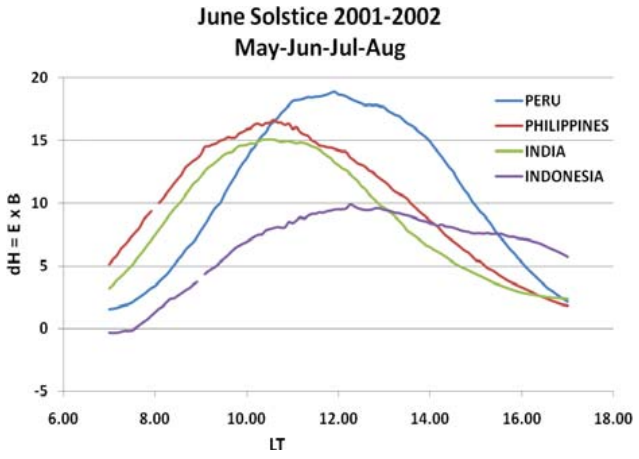

Fig. 4a. Same as Fig. 3a for June solstice.

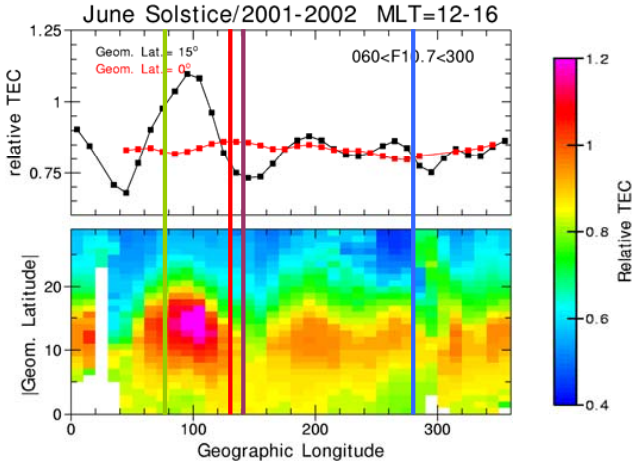

Fig. 4b. Same as Fig. 3b for June solstice.

Comparisons for the December solstice are displayed in Fig. 5. The 4-cell pattern no longer exists and has been replaced by a 3-cell pattern. While Figs. 3 and 4 clearly show that the magnetometer-inferred $E \times B$ drift velocities are capable of explaining the TOPEX/TEC crest separation in the four longitude sectors for Equinox and June solstice conditions, the comparison for the December solstice season displayed in Fig. 5 is somewhat ambiguous. Clearly the $E \times B$ drifts in the Philippine sector are greater than in the Peruvian sector and this accounts for the greater crest separation seen in the TOPEX/TEC observations between these two sectors. What needs further investigation is why the $E \times B$ drift velocities in the Indonesian and Indian sectors seem to be lower than in the Philippine sector, while the TEC crest separation appears to be equivalent to the Philippine sector. Interestingly, there now exists a gradient in TEC between Peruvian and the East Brazilian/Atlantic sector. Since appropriately-placed magnetometers in the Eastern Brazilian sector were not available, daytime $E \times B$ drift velocities could not be compared with the Peruvian values.

4 Conclusions and future work

The results presented in Figs. 3, 4 and 5 are unique and the comparisons between ground-based, inferred $E \times B$ drift velocities and the satellite TEC observations that relate to the 4-cell pattern and its seasonal and longitudinal dependence have not previously been compared and open the opportunity to research three, fundamentally-important and specific scientific questions. 1.) How sharp are the longitude gradients in daytime, vertical $E \times B$ drift velocities that define the boundaries of each of the 4 cells? 2.) Is the 4-cell pattern in $E \times B$ drifts observed on a-day-to-day basis? and 3.) Are current, state-of-the-art theoretical models capable

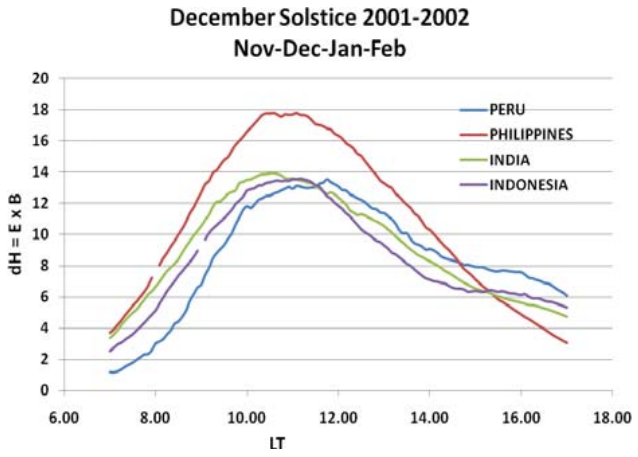

Fig. 5a. Same as Fig. 3a for December solstice.

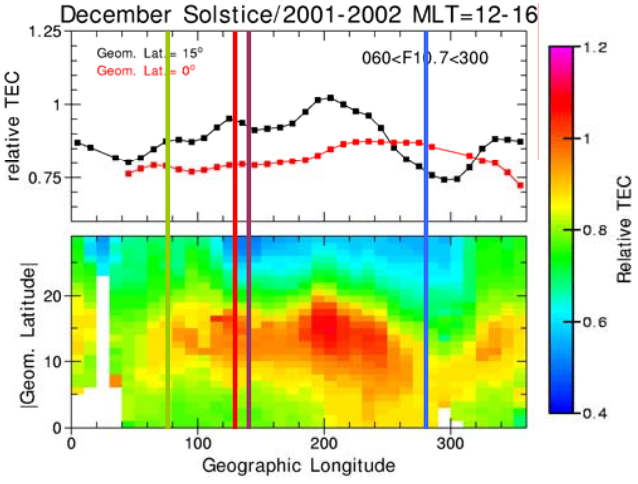

Fig. 5b. Same as Fig. 3b for December solstice.

of reproducing the sharpness of the boundaries in daytime, vertical $E \times B$ drift velocities?

Question 1.) As demonstrated in the previous section (Fig. 3a), the observed difference between the maximum $E \times B$ drift velocity in the Philippine sector (23 m/s) and the Indonesian sector (15 m/s) is (23–15) or 8 m/s. This is across 15° longitude or about 0.5 m/s/degree. Answering this question from an observational standpoint will set the "benchmarks" that are needed by the theoretical modelers to understand the physical mechanisms and to compare model results with observations.

Question 2.) To date, all of the multi-technique observations of the 4-cell pattern have been "averages" – typically a month-long average. Establishing if the 4-cell pattern exists on a day-to-day basis will help to determine whether the identified mechanism, the latent heat release in the tropospheric regions, is acting on a day-to-day basis.

Question 3.) If the state-of-the-art theoretical models are capable to capture the gradients, then the model results can be analyzed to determine the causes of the sharp boundaries and their longitude dependence.

C/NOFS' Ion Velocity Meter (IVM) and Vector Electric Field Instrument (VEFI) sensors could be used to obtain the daytime, vertical $E \times B$ drift velocities at the magnetic equator as a function of longitude, local time and season. The IVM sensor measures the $E \times B$ drift velocity perpendicular to B, and can be used to obtain the vertical $E \times B$ drifts at the magnetic equator by mapping along the geomagnetic field line. The VEFI sensor measures the electric field component perpendicular to B and can be similarly mapped to the magnetic equator.

The theoretical model that could be used to address these specific science questions has been described in a paper by Fuller-Rowell et al. (2008), which was developed to demonstrate the impact of terrestrial weather on the upper atmosphere. The Integrated Dynamics through Earth's Atmosphere (IDEA) model consists of the Whole Atmosphere Model (WAM) and a Global Ionosphere Plasmasphere (GIP) model.

Acknowledgements. We thank Jorge Chau, Director of the Jicamarca Radio Observatory, Peru for providing the Jicamarca and Piura magnetometer observations; Kiyo Yumoto, Director of the Space Environment Research Center, Kyushu University, Japan for the Davao, Muntinlupa, Yap and Biak magnetometer observations; and Archana Bhattacharyya, Director of the Indian Institute of Geomagnetism, India for the Thirunelveli and Alibag magnetometer observations. This work was supported by the NASA Heliophysics Theory program.

Topical Editor K. Kauristie thanks J. Retterer and two other anonymous referees for their help in evaluating this paper.

References

Anderson, D. N.: A theoretical study of the ionospheric, F-region equatorial anomaly, I. Theory, Planet. Space Sci., 21, 409–419, 1973.

Anderson, D., Anghel, A., Yumoto, K., Ishitsuka, M., and Kudeki, E.: Estimating daytime vertical $E \times B$ drift velocities in the equatorial F-region using ground-based magnetometer observations, Geophys. Res. Lett., 29(12), 1596, doi:10.1029/2001GL014562, 2002.

Anderson, D., Anghel, A., Chau, J., and Veliz, O.: Daytime vertical $E \times B$ drift velocities inferred from ground-based magnetometer observations at low latitudes, Space Weather, 2, S11001, doi:10.1029/2004SW000095, 2004.

Anderson, D., Anghel, A., Chau, J., and Yumoto, K.: Global, low-latitude, vertical $E \times B$ drift velocities inferred from daytime magnetometer observations, Space Weather, 4, S08003, doi:10.1029/2005SW000193, 2006.

England, S. L., Maus, S., Immel, T. J., and Mende, S. B.: Longitudinal variation of the E-region electric fields caused by atmospheric tides, Geophys. Res. Lett., 33, L21105, doi:10.1029/2006GL027465, 2006.

Fejer, B. G., Jensen, J. W., and Su, S.-Y.: Quiet time equatorial F region vertical plasma drift model derived from ROCSAT-1 observations, J. Geophys. Res., 113, A05304, doi:10.1029/2007JA012801, 2008.

Forbes, J. M., Zhang, X., Palo, S., Russell, J., Mertens, C. J., and Mlynczak, M.: Tidal variability in the ionospheric dynamo region, J. Geophys. Res., 113, A02310, doi:10.1029/2007JA012737, 2008.

Fuller-Rowell, T. J., Akmaev, R. A., Wu, F., Anghel, A., Maruyama, N., Anderson, D. N., Codrescu, M. V., Iredell, M., Moorthi, S., Juang, H.-M., Hou, Y.-T., and Millward, G.: Impact of terrestrial weather on the upper atmosphere, Geophys. Res. Lett., 35, L09808, doi:10.1029/2007GL052911, 2008.

Hagan M. E. and Forbes, J. M.: Migrating and non-migrating diurnal tides in the middle and upper atmosphere excited by tropospheric latent heat release, J. Geophys. Res., 107(D24), 4754, doi:10.1029/2001JD001236, 2002.

Hanson, W. B. and Moffett, R. J.: Ionization transport effects in the equatorial F region, J. Geophys. Res., 71, 5559–5572, 1966.

Immel, T. J., Sagawa, E., England, S. L., Henderson, S. B., Hagan, M. E., Mende, S. B., and Frey, H. U.: Control of equatorial ionospheric morphology by atmospheric tides, Geophys. Res. Lett., 33, L15108, doi:10.1029/2006GL026161, 2006.

Lin, H., Hsiao, C. C., Liu, I. Y., and Liu, C. H.: Longitudinal structure of the equatorial ionosphere: Time evolution of the four-peaked EIA structure, J. Geophys. Res., 112, A12305, doi:10.1029/2007JA12455, 2007.

Kil, H., Oh, S.-J., Kelley, M. C., Paxton, L. J., England, S. L., Talaat, E., Min, K.-W., and Su, S.-Y.: Longitudinal structure of the vertical $\boldsymbol{E}\times\boldsymbol{B}$ drift and ion density seen from ROCSAT-1, Geophys. Res. Lett., 34, L14110, doi:10.1029/2007GL030018, 2007.

Sagawa, E., Immel, T. J., Frey, H. U., and Mende, S. B.: Longitudinal structure of the equatorial anomaly in the nighttime ionosphere observed by IMAGE/FUV, J. Geophys. Res., 110, A11302, doi:10.1029/2004JA010848, 2005.

Scherliess, L. and Fejer, B. G.: Radar and satellite global equatorial F region vertical drift model, J. Geophys. Res., 104, 6829–6842, 1999.

Scherliess, L., Thompson, D. C., and Schunk, R. W.: Longitudinal variability of low-latitude total electron content: Tidal influences, J. Geophys. Res., 113, A01311, doi:10.1029/2007JA012480, 2008.